

# SAMPLING RELATED ISSUES IN POD-BASED MODEL REDUCTION OF SIMPLIFIED CIRCULATING FLUIDISED BED COMBUSTOR MODEL

Katarzyna Bizon\*

Institute of Chemical and Process Engineering, Cracow University of Technology, ul. Warszawska  
24, 31-155 Kraków, Poland

Over the last decades the method of proper orthogonal decomposition (POD) has been successfully employed for reduced order modelling (ROM) in many applications, including distributed parameter models of chemical reactors. Nevertheless, there are still a number of issues that need further investigation. Among them, the policy of the collection of representative ensemble of experimental or simulation data, being a starting and perhaps most crucial point of the POD-based model reduction procedure. This paper summarises the theoretical background of the POD method and briefly discusses the sampling issue. Next, the reduction procedure is applied to an idealised model of circulating fluidised bed combustor (CFBC). Results obtained confirm that a proper choice of the sampling strategy is essential for the modes convergence however, even low number of observations can be sufficient for the determination of the faithful dynamical ROM.

**Keywords:** model reduction, proper orthogonal decomposition, circulating fluidised bed, optimal sampling

## 1. INTRODUCTION

The continuous advancements observed with computing power and hardware storage capacities available nowadays to researchers permit to handle detailed numerical simulation of mathematical models and to analyse efficiently the resulting massive data. Still, there is a demand for the development and improvement of model order reduction techniques (Lucia et al., 2003). Especially when it comes to real-time control applications, that require the use of fast and accurate models, or for detailed analysis of distributed dynamical models, e.g. chemical reactor models. The latter, usually given in the form of infinite-dimensional partial differential equations (PDEs), for practical considerations, have to be first reduced to a finite-dimensional dynamical system. Typically, this step is accomplished by numerical discretisation of spatial differential operators, yielding a system of ordinary differential equations (ODEs), to be then integrated in time using an appropriate numerical scheme. Classical discretisation methods, such as finite differences or finite elements, are relatively simple to apply, yet they produce large sets of ODEs which may be difficult to handle. Model reduction consists of finding a low-dimensional approximation for such systems. The reduction procedure is customarily accomplished by projection of the governing equations onto a suitable subspace. Projection methods, and particularly the Galerkin projection method (Hesthaven et al., 2007), permits to find low order yet accurate description of the original PDEs, provided that a proper choice of the functional basis is made. Considering that classical basis may fail to predict correctly the solution, as it happens in the case of the functional approximation of saw-tooth function

\* Corresponding author, e-mail: kbizon@chemia.pk.edu.pl

using Fourier series (Hesthaven et al., 2007), the alternative is to build an *empirical basis* arising directly from the (simulated) behaviour of the system. Such basis can be identified by means of a method of proper orthogonal decomposition (POD), which, based on set of observations describing spatiotemporal behaviour of the model, determines a set of optimal orthonormal functions (Holmes et al., 1996) for the given problem. When it comes to the order reduction of the evolutionary PDEs, such observations – spatial profiles of the solution collected over time, also called *snapshots* – generally originate from the numerical simulation of the model obtained using classical discretisation schemes, to which we will refer to as the full order model (FOM). It should be noted that, once the snapshots are obtained, the POD is a merely algebraic linear procedure, in which the governing equations and boundary conditions do not come into play. Hence, it would be natural to think to exploit the degree of freedom consisting of the choice of the snapshots to be employed for the generation of the ROM, in order to obtain the best performing ROM for a given number of reduced variables, or conversely obtain the minimum number of variables necessary to achieve a given accuracy. In general, the lower the number of snapshots, the lower the computing time and storage needs. In this view, the sampling of the snapshots, being the very first step, is most crucial for accuracy of the reduced order model (ROM) to be determined. While the exploration of the parameter space is a well established policy for the generation of a global POD i.e. able to capture correctly the overall dynamics of the system as the parameters vary (Zhang et al., 2003), still not much has been done in terms of the influence of the total number of snapshots employed, or their temporal distribution, on the ROM performance.

In this study, the POD based reduction procedure, together with sampling-related issues, is illustrated on a relatively simple one-dimensional dynamical model of circulating fluidised bed combustor (CFBC) under isothermal operation (Bizon and Continillo, 2009; Bizon and Continillo, 2012). Apparently, in parallel to the spread of commercial applications of CFBC technology, a number of models and software tools has been developed (Basu, 1999). Their level of sophistication is growing steadily, not only in terms of the number of the dimensions – from zero-dimensional (Lombardi et al., 2013) to three-dimensional models (Lu et al., 2013) – but also in terms of the considered phenomena. Yet, while complex three-dimensional models based on the Navier-Stokes equations found their application in the development of new reactor design, the simple dynamical model is irreplaceable for the detailed steady-state and dynamical analysis of system behaviour. This involves a global evaluation of the influence of the operational parameters at steady operation, i.e. excess air, fluidisation velocity, fluid properties, and many others; or dynamic prediction of the system response to sudden changes of process conditions, e.g. fuel feed rate. Despite the simplicity of the CFBC model proposed here, the solution of the FOM still remains quite expensive in terms of computational time, and is expected to increase when adding an unsteady energy balance equation. Hence, detailed model analysis and its successive phenomenological extension still necessitates the construction of a light yet faithful ROM.

## 2. MODEL OF CIRCULATING FLUIDISED BED COMBUSTOR

With reference to the classical reactor theory, the circulating fluidised bed combustor (CFBC) system (Fig. 1) is viewed here as a plug flow tubular heterogeneous reactor, followed by a gas-solid separator (cyclone) and a loop-seal modeled as a continuously stirred tank (CST).

The proposed dynamical model, based on the framework presented in Barletta et al. (2003), is isothermal in the present formulation and integrates a simplified fluid dynamics with a quasi-steady approximation made for inter-phase momentum exchange. The riser is subdivided vertically into two zones that is a dense bed present at the bottom and a dilute region above it, the latter composed of a splashing zone and a freeboard. Both volatile matter and ash content of the fuel are neglected, therefore combustion modelling is simplified to a single one-step heterogeneous reaction ( $C + O_2 \rightarrow CO_2$ ). More details concerning the model assumptions, constitutive relationships and correlations used in the model formulation can be found in (Bizon and Continillo, 2009; Bizon and Continillo, 2012).

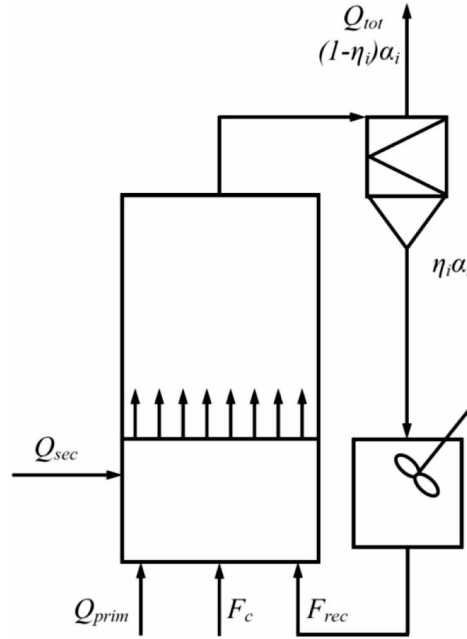


Fig. 1. Scheme of CFBC with indicated flow pattern/recycle of the process streams

The fuel population balance equation is simplified by lumping fixed carbon into so-called *coarse char* particles, fed into the combustor, and *fine char*, generated by combustion-assisted attrition of coarse char. Hence, in the dimensionless form, the mass balance equations for solid phase can be written as:

$$\frac{\partial \alpha_c}{\partial \tau} + \frac{\partial (v_c \alpha_c)}{\partial x} = -\sigma_a \alpha_c - \sigma_c \alpha_c \quad (1)$$

$$\frac{\partial \alpha_f}{\partial \tau} + \frac{\partial (v_f \alpha_f)}{\partial x} = \sigma_a \alpha_c - \sigma_f \alpha_f \quad (2)$$

where  $\alpha_i$  and  $v_i$  are, respectively, the dimensionless suspension density and the velocity of the coarse ( $i = c$ ) and fine ( $i = f$ ) fraction of the char, respectively, while  $\sigma_i$  denotes a dimensionless consumption rate: due to attrition,  $\sigma_a$ , and due combustion of coarse and fine particles –  $\sigma_c$  and  $\sigma_f$ . The associated boundary conditions are:

$$v_c(0, \tau) \alpha_c(0, \tau) = \kappa_1 F_c - F_{rec} \alpha_{c,rec}(\tau) \quad (3)$$

$$v_f(0, \tau) \alpha_f(0, \tau) = F_{rec} \alpha_{f,rec}(\tau) \quad (4)$$

where  $F_c$  is a dimensionless fed mass flow rate of the coarse particles, while  $F_{rec}$  is a mass flow rate of recycled solids. The densities of recycled solids,  $\alpha_{i,rec}$ , are calculated from the CST mass balance:

$$\frac{\partial \alpha_{c,rec}}{\partial \tau} = \kappa_2 [\eta_c v_c(1, \tau) \alpha_c(1, \tau) - F_{rec} \alpha_{c,rec}] \quad (5)$$

$$\frac{\partial \alpha_{f,rec}}{\partial \tau} = \kappa_2 [\eta_f v_f(1, \tau) \alpha_f(1, \tau) - F_{rec} \alpha_{f,rec}] \quad (6)$$

where  $\eta_i$  denotes cyclone efficiency. Finally, the mass balance for carbon dioxide with the associated boundary condition is:

$$\frac{\partial (\varepsilon \alpha_{CO_2})}{\partial \tau} + \frac{\partial (v_g \varepsilon \alpha_{CO_2})}{\partial x} = \sigma_c \alpha_c + \sigma_f \alpha_f \quad (7)$$

$$\alpha_{CO_2}(0, \tau) = 0 \quad (8)$$

The void fraction  $\varepsilon$  and the corresponding velocity profiles  $v_i$  are calculated from a steady state fluid dynamic model. The model distinguishes a primary and a secondary air stream, both entering at ambient temperature. However to avoid discontinuities in the spatial domain, in this demonstrative study only the primary air flow is considered, therefore  $Q_{sec} = 0$ . In all simulations, the initial profiles of solid suspension densities and carbon dioxide concentration are set to be equal zero. To provide a general insight into the physics of the presented results, the basic (dimensional) parameters used in this study are collected in Table 1.

Table 1. Basic parameters used in the reference simulation

|   |      |
|---|------|
| Coarse char cyclone efficiency, $\eta_c$        | 1    |
| Fine char cyclone efficiency, $\eta_f$          | 0.9  |
| Coarse particle diameter, $d_c$ [mm]            | 3    |
| Fine particle diameter, $d_f$ [ $\mu\text{m}$ ] | 100  |
| Bed particle diameter, $d_b$ [ $\mu\text{m}$ ]  | 300  |
| Fluidisation velocity, $u_0$ [m/s]              | 5    |
| Temperature, $T$ [K]                            | 1123 |
| Excess air factor, $\lambda$                    | 1.2  |

### 3. MODEL REDUCTION TECHNIQUE

#### 3.1. Proper orthogonal decomposition

The aim of the POD method is to decompose any given ensemble of data into an *optimal*, in the sense of  $L^2$  norm, set of orthogonal *basis functions* or *modes*. Denote by  $u(\mathbf{x}, t_i)$  a scalar field of numerical or experimental observations, where  $\mathbf{x}$  is an  $N$ -dimensional vector and  $t_i, i = 1, \dots, M$  represents sampling time instances. It can be demonstrated (Holmes et al., 1996) that the POD basis  $\{\phi_n(\mathbf{x})\}_{n=1}^N$  can be obtained by solving the eigenvalue problem:

$$\mathbf{K}\phi = \lambda\phi \quad (9)$$

where  $\mathbf{K} \in \mathfrak{R}^N \times \mathfrak{R}^N$  is an autocorrelation matrix of dimension  $N$ , defined as:

$$\mathbf{K}(\mathbf{x}, \mathbf{y}) = \langle u(\mathbf{x}, t_i) u^T(\mathbf{y}, t_i) \rangle \quad (10)$$

with  $\langle \cdot \rangle$  denoting ensemble average over the number of samples  $M$ . Apparently, each eigenfunction  $\phi_n$  is associated with the eigenvalue  $\lambda_n$ ; the ordering of the eigenvalues from the largest to the smallest induces and ordering of the corresponding functions, from the most to the least important. A very common practice is to use then a so-called *cumulative correlation energy* captured by the  $K$  leading modes, defined as:

$$E_K = \frac{\sum_{n=1}^K \lambda_n}{\sum_{n=1}^N \lambda_n} \quad (11)$$

as a criterion for the determination of the *truncation degree*  $K$  of the POD reduced order model. Once determined the value  $K$  (e.g. by taking the value for which  $E_k > 99\%$ ), the solution  $u(\mathbf{x}, t_i)$  can be expressed, in a truncated form, as:

$$u(\mathbf{x}, t_i) \approx \sum_{n=1}^K a_n(t_i) \phi_n(\mathbf{x}) \quad (12)$$

where  $K \ll N$  is a truncation order, whereas  $a_n, n = 1, \dots, K$  are modal coefficients that can be determined by the orthogonal projection of the field  $u(\mathbf{x}, t_i)$  onto the basis, i.e.:

$$a_n(t_i) = (u(\mathbf{x}, t_i), \phi_n(\mathbf{x})) \quad (13)$$

where  $(\cdot, \cdot)$  is the inner product, or solving the ODEs system resulting from the Galerkin projection of the FOM onto the basis (more details in the Subsection 3.2).

When the number of gridpoints  $N$  is very large (e.g. when dealing with observations coming from CFD simulations), both storage and calculation requirements of the eigenvalue problem defined by Eq. (9) become very high, hence the above described approach (denoted sometimes as *direct method*) becomes impractical or even out of question. In case of  $N \gg M$ , the use of an alternative approach, called also *method of snapshots* or *strokes* (Sirovich, 1987), becomes preferable, as it permits to reduce the size of the eigenvalue problem that has to be solved from  $N$  to  $M \ll N$ . In particular, Sirovich (1987) demonstrated that the eigenfunctions  $\phi_n$  can be written as a linear combination of the given scalar field, that is:

$$\phi_n(\mathbf{x}) = \sum_{i=1}^M \psi_n(t_i) u(\mathbf{x}, t_i) \quad (14)$$

Where  $\psi_n$  can be obtained from:

$$\mathbf{C} \psi = \lambda \psi \quad (15)$$

where  $\mathbf{C} \in \mathfrak{R}^M \times \mathfrak{R}^M$  is defined as:

$$\mathbf{C}(\mathbf{x}, \mathbf{y}) = \langle u^T(\mathbf{x}, t_i) u(\mathbf{y}, t_i) \rangle \quad (16)$$

The use of the method of snapshots yields results almost identical – up to the machine accuracy – to those obtained by the direct method.

### 3.2. Galerkin method

Consider the problem of spatiotemporal evolution of the quantity  $u(x, t)$  represented by a PDE of the form (Hesthaven et al., 2007):

$$\frac{\partial u}{\partial t} = D(u), \quad x \in [a, b], \quad t \geq 0 \quad (17)$$

$$B_L(u(a, t)) = g, \quad B_R(u(b, t)) = h, \quad t \geq 0 \quad (18)$$

$$u(x, 0) = f(x), \quad x \in [a, b], \quad t = 0 \quad (19)$$

where  $D$  is a non-linear operator that may involve spatial derivatives of the dependent variable  $u$ , while  $B_L$  and  $B_R$  are the boundary operators. In spectral methods, and in particular in Galerkin method, the solution is sought in the form:

$$u_K(x, t) = \sum_{n=1}^K a_n(t) \phi_n(x) \quad (20)$$

where  $\phi_n(x)$  are elements of a known, prescribed *a priori*, orthonormal spatial basis  $\{\phi_n(x)\}_{n=1}^N$ . The unknown temporal coefficients  $a_n(t)$ ,  $n = 1, \dots, K$ , are obtained by requiring the residual:

$$R_K(x, t) = \frac{\partial u_K(x, t)}{\partial t} - Du_K(x, t) \quad (21)$$

to be orthogonal to the basis, that is:

$$(R_K(x, t), \phi_m(x)) = 0, \quad m = 1, \dots, K \quad (22)$$

From the orthonormality of the basis functions, in this particular case the POD modes, with respect to the chosen inner product  $(\cdot, \cdot)$  this procedure yields a low-dimensional system of ODEs consisting of  $K$  equations, namely:

$$\frac{\partial a_m}{\partial t} = \left( D \left( \sum_{n=1}^K a_n \phi_n \right), \phi_m \right), \quad n, m = 1, \dots, K \quad (23)$$

with the initial condition determined by the orthogonal projection of the PDEs' initial condition given by Eq. (19) on to the basis, i.e.:

$$a_m(0) = (f, \phi_m), \quad m = 1, \dots, K \quad (24)$$

The number of ODEs,  $K$ , defined by Eq. (23), is much smaller than  $N$ , where  $N$  denotes the number of ODEs arising from the discretisation of the PDEs using some standard approach, for example finite difference or finite element method.

### 3.3. Sampling problem

It is evident that the choice of the approach – the direct method or the snapshots method – is determined by the form, i.e. size, of the data set available. If the observations  $u(\mathbf{x}, t_i)$  consists of a long time history with low spatial resolution, which is typical of coarse numerical simulations or experimental data collected employing a limited number of sensors (Rajat and Yogendra, 2013), the application of the direct method is appropriate. On the other hand, for data with a moderate time history but high spatial resolution, e.g. data resulting from high-dimensional numerical simulation (Hekmati et al., 2011) or experimental measurements characterised by high spatial resolution, for instance performed by optical imaging (Bizon et al., 2010), the method of snapshots becomes favourable. In the second case, while the spatial dimension  $N$  is imposed by the computational grid or the camera resolution, both the choice the number  $M$  of the observations and their temporal distribution are rather arbitrary. It is well known that important dynamics must be contained in the snapshots (Rowley et al., 2001); yet, the choice of the optimal number of snapshots and the sampling time step are open questions.

According to Breuer and Sirovich, 1991, the number of snapshots  $M$  can be roughly estimated on the basis of the convergence of the discrete eigenspectrum  $\lambda_n$  to the continuous eigenspectrum  $\lambda_n^\infty$ , or to the discrete eigenspectrum obtained for  $M^\infty \rightarrow \infty$ .

A similar approach, based on the convergence of the POD modes, was introduced in Hekmati et al., 2011, measured in terms of a correlation coefficient defined as:

$$\rho_n^M = \frac{\langle \phi_n^M \phi_n^\infty \rangle}{\sqrt{\langle \phi_n^\infty \phi_n^\infty \rangle \langle \phi_n^M \phi_n^M \rangle}} \quad (25)$$

where  $\phi_n^\infty$ , denotes the  $n$ -th mode of the reference case (calculated with  $M^\infty \rightarrow \infty$ ) while  $\phi_n^M$  denotes the  $n$ -th mode of test case ( $M \ll M^\infty$ ).

#### 4. RESULTS AND DISCUSSION

In order to obtain a high-fidelity solution of the system described by Eqs. (1-8), fundamental for the determination of the POD basis and required as a reference in the evaluation of the method performance, in the first step the FOM was constructed. To this aim, system of PDEs describing mass balances in the riser of the CBFC loop was first approximated in space by means of finite differences with staggered grid, employing  $N = 500$  spatial nodes. Then, the Adams-Moulton implicit method with time-adaptive integration step was used to solve system of 1500 ODEs resulting from the discretisation, together with two ODEs describing coarse and fine fractions of the char in the CST placed in the solid recycle loop (see Fig. 1).

Figure 2 shows representative snapshots of the coarse (Fig. 2a) and fine (Fig. 2b) char concentration, being an input for the POD procedure. It can be noted that the coarse char suspension density profile is decreasing along the riser height (Fig. 2a). This is clearly the result of the coarse char consumption due to combustion and attrition. In the bottom bed zone (up to  $x = 0.1$ ) char density values are very high, as an outcome of much lower particle velocities and limited diffusion of oxygen. This is due to the presence of the dense matrix of inert bed material. Char density decreases drastically right above the dense bed. Moreover, in the early transient, coarse char concentration close to the feed port, i.e. at the bottom of the reactor, remains almost constant ( $\alpha_c(0) \approx 1.2 \cdot 10^{-3}$ ) since the presence of coarse particles in this zone results only from the feed of fresh fuel particles. As soon as the recycle of unburned fuel initiates, depending on particle residence time both in the riser and loop-seal modeled as a continuous stirred tank, it starts to increase and eventually, at steady state, approximately doubles its value ( $\alpha_c(0) = 2.44 \cdot 10^{-3}$ ). Further, the suspension density profiles of fines (Fig. 2b) reflect a competition of two processes – fines generation due to coarse char attrition and successive fines burn-out. In the early transient, this competition reveals through the presence of a single concentration peak, in the correspondence of the upper part of the dense zone. Then, at steady state, a second peak can be observed in the correspondence of the reactor inlet, resulting from the recycle of unburned fines.

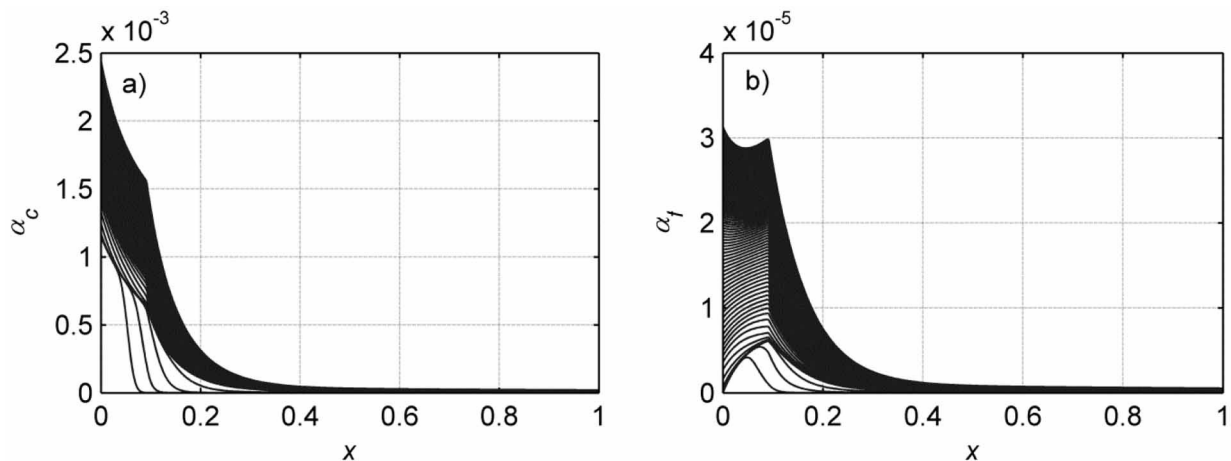


Fig. 2. Snapshots of coarse (a) and fine char concentration (b) obtained from FOM simulations

A question that need to be answered now is: what should be the ensemble size used in the POD procedure, keeping in mind that the objective is to minimise the approximation error of the resulting ROM, without neglecting the computational cost of the determination of the basis. Remember that the number of snapshots  $M$  will affect the computational complexity of the matrix multiplication (Eq. 10) in the direct approach, and the size of the eigenvalue problem (Eq. 15) to be solved in the method of snapshots. Hence, recalling the issue of eigenvalue spectra convergence (Breuer and Sirovich, 1991), the POD is performed, separately for each state variable, on ensembles of different sizes, varying from  $M = 25$  and  $M = 2500$  (the latter adopted as a reference value). Each data ensemble consists of snapshots equally spaced in time, from transient and steady state. Although a similar criterion for the choice of  $M$  has been previously adopted in Bizon and Continillo (2009), where the behaviour of the ROM in the early transient was investigated, the relationship between the number of snapshots and approximation error of the ROM was not investigated further.

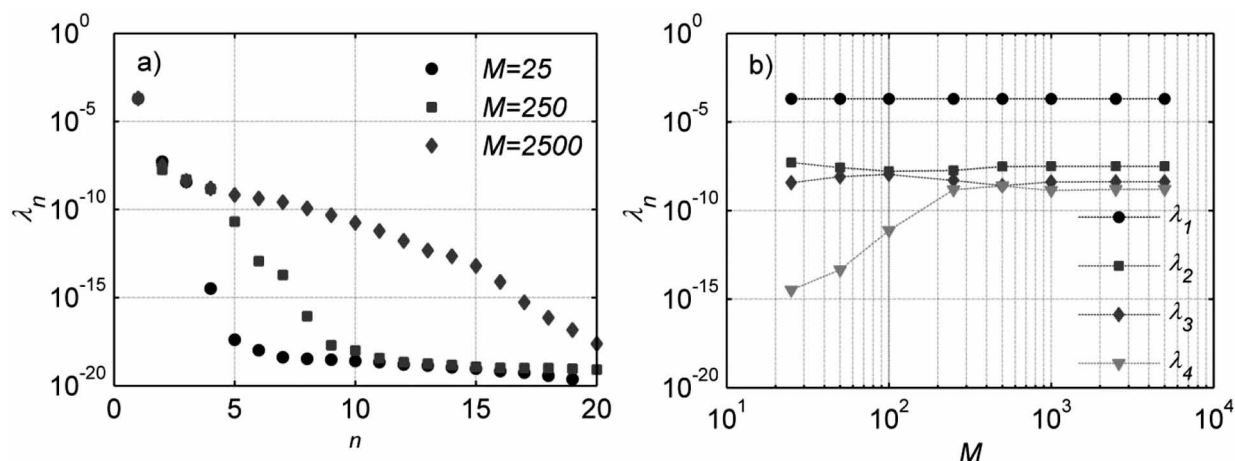


Fig. 3. Eigenvalue spectrum of coarse char concentration for different number of snapshots (a) and leading four eigenvalues as a function of the number of snapshots (b).

Figure 3a shows the initial parts of representative eigenspectra (for  $M=25$ ,  $M=250$  and  $M=2500$ ) of the POD modes determined for coarse particles. Fast descent of the spectra indicates that, as a result of the low spatiotemporal complexity of the solution, a very small number of leading modes is carrying significant information: indeed, for each state variable and for each sampling strategy, the cumulative energy of the first mode,  $E_1$  defined by Eq. (11) is already higher than 99%. Also, when  $M$  increases, the computed spectrum approaches the reference spectrum, i.e. the one determined using as many as 2500 snapshots.

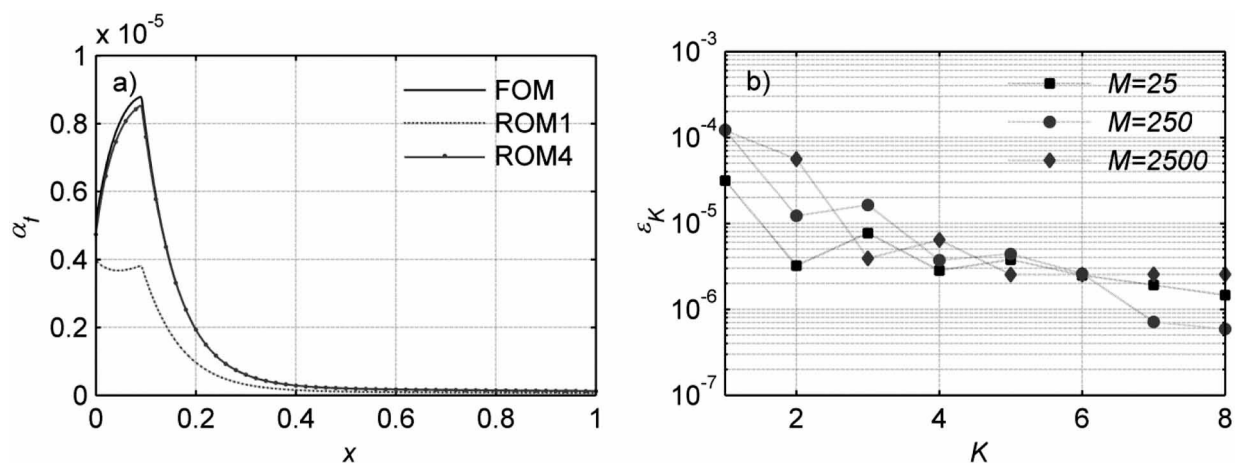


Fig. 4. Comparison of the axial concentration of fine char at time  $\tau = 50$  obtained using FOM, ROM1 and ROM4 (a) and comparison of the error on the fine char concentration for  $M = 25, 250$  and  $2500$

Despite of a very high energy content in the first mode, the ROM constructed by means of the Galerkin projection of the FOM onto the first mode only (for each state variable), denoted as ROM1 in Fig. 4a, fails completely to predict the transient behaviour of the system. It is therefore necessary to add higher order modes to capture the model behaviour in the entire time interval of interest. Indeed, only the steady state approximation of the solution obtained by ROM1 (not reported here) can be considered as acceptable, even though obtained with only 5 ODEs instead of 1502: three resulting from the projection of PDEs onto first POD modes and two describing the mass balance of the CST present in the recycle loop. Adding more modes in reduced order approximation results in much higher, even in the early transient, accuracy (ROM4 in Fig. 4a).

Considering again the eigenspectra evaluated previously (Figure 3) one could conclude that several hundreds of snapshots should provide convergence of the leading eigenvalues and hence a faithful POD basis. However this is not confirmed by another criterion, i.e. correlation coefficient of POD modes. In fact, only the first modes  $-\rho_1^{25} = 0.999$  and  $\rho_1^{250} = 0.999$  for each state variable – appear not to be affected by the sampling policy (Table 2).



Table 2. Correlation coefficient  $\rho_n^M$  of POD modes

|         | Coarse char, $\alpha_c$ |           | Fine char, $\alpha_f$ |           | CO <sub>2</sub> , $\alpha_{CO_2}$ |           |
|---------|-------------------------|-----------|-----------------------|-----------|-----------------------------------|-----------|
|         | $M = 25$                | $M = 250$ | $M = 25$              | $M = 250$ | $M = 25$                          | $M = 250$ |
| $n = 1$ | 0.9999                  | 0.9999    | 0.9999                | 0.9999    | 0.9999                            | 0.9999    |
| $n = 2$ | 0.2220                  | 0.9465    | 0.9993                | 0.9992    | 0.9953                            | 0.9919    |
| $n = 3$ | 0.1208                  | 0.3461    | 0.9651                | 0.4102    | 0.8749                            | 0.9868    |

Hence, to provide an overall measure of the effect of the sampling policy, an average relative least-square truncation error is defined as:

$$\varepsilon_K = \left\langle \frac{1}{N} \frac{\left\| u(\mathbf{x}, t_i) - \sum_{n=1}^K a_n(t_i) \psi_n(\mathbf{x}) \right\|^2}{\left\| u(\mathbf{x}, t_i) \right\|^2} \right\rangle \quad (27)$$

where  $K$  denotes truncation order, i.e. number of modes employed in the approximation, whereas  $\sum_{n=1}^K a_n(t_i) \psi_n(\mathbf{x})$  is the approximated solution, with  $a_k(t_i)$  determined by solving the ROM in the form of dynamical ODEs defined by Eq. (23). Unlike the projection method defined by Eq. (13) and used by Brenner et al. (2012) in the evaluation of the sampling strategy onto the ROM performance, the error calculated for the solution obtained from dynamic ROM determined by Galerkin projection accounts not only for the effect of spatial approximation but also numerical integration (e.g. time lag with respect to FOM).

It is interesting to examine now the values of the error of the solution obtained from the ROM employing the reference basis ( $M = 2500$ ) and the basis determined from very low number of observations ( $M = 25$ ). As it can be seen in Figure 4b, showing the average relative least-square error for fine char, except for the very first value of  $K$  (i.e. 1 and 2), the values of  $\varepsilon_K$  are not influenced by the sampling policy. This could be surprising, however one should remember that both basis employed here have still empirical character. Moreover, while use of very high resolution data is out of question in calculation of the modal coefficient by means of the projection of the data onto basis (Eq. (13)), relatively low number of observations  $M$  can be sufficient to determine the basis, which combined with adequate choice of integration procedure delivers fast and faithful dynamic ROM. Thus, in choice of sampling strategy the intrinsic optimality of the POD should be unified with model generality: less data may in fact deliver more generic and more stable modes, not overloaded by redundant information or, for example, by linearly dependent observations.

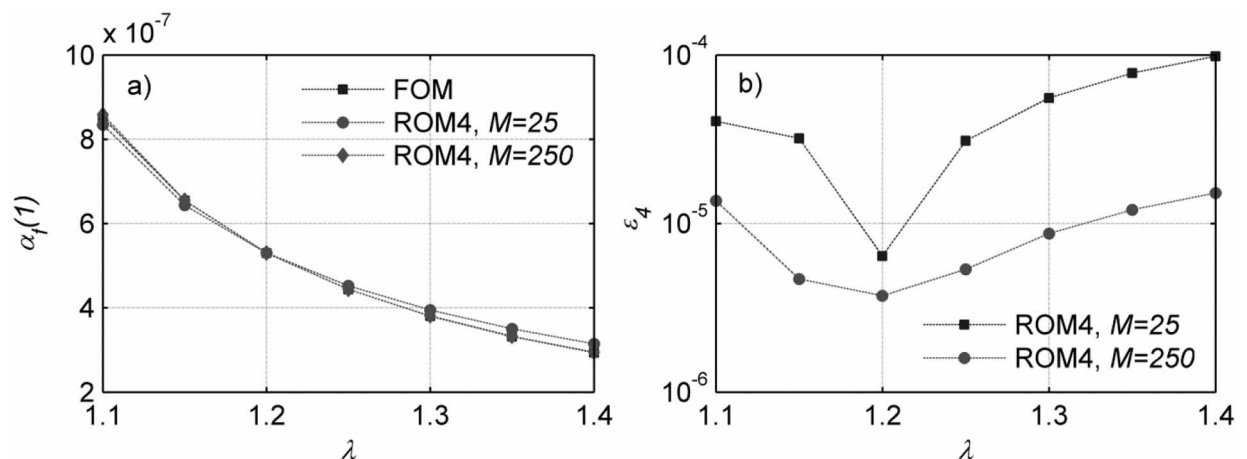


Fig. 5. Comparison of fine char concentration at steady state at the outlet (a) and average relative least-square truncation error (b) as a function of excess air ratio

The last part of this study concerns the validity of the determined POD bases at off-reference conditions, i.e. when model parameters vary. Both dynamic and steady state behaviour of the system is considered. In general, by reason of its empirical origin, the ROM determined by the projection of the FOM onto the POD basis determined from the unique solution is not expected to be valid over too wide a range of operating conditions, especially when parameter variations lead to qualitative changes of the system behaviour, e.g. occurrence of bifurcation. But again, there is no systematised snapshot generation procedure that could provide a universal POD basis, except for some *ad hoc* procedures in which certain *global* bases are obtained from a combination of data originating from different simulations, conducted for different values of the key parameter.

Figure 5a shows the effect of the variation of the excess air ratio,  $\lambda$ , on the concentration of unburned fines at the outlet. In order to adjust the value of  $\lambda$  the fuel feed rate was varied, while keeping constant all other parameters. Starting from relatively high values of  $\alpha_f(1)$  for near stoichiometric condition ( $\lambda = 1.1$ ), the combustion efficiency improves with increasing excess air ratio. However as expected, this improvement becomes less significant above 20% excess air. Comparing the outlet values obtained using FOM and ROMs, it can be observed that, whilst the ROM built from 250 snapshots follow the FOM solution over the entire explored range of  $\lambda$ , the one obtained from 25 snapshots profiles visibly deviates from the FOM at off-reference conditions. This effect is even better reflected by the error values shown in Figure 5b – the error of the ROM exhibits a characteristic minimum at the reference value ( $\lambda = 1.2$ ) of the excess air ratio, at which the solution was sampled to build the basis, and tends to increase when the value of  $\lambda$  changes, yet, it has acceptable order of magnitude.

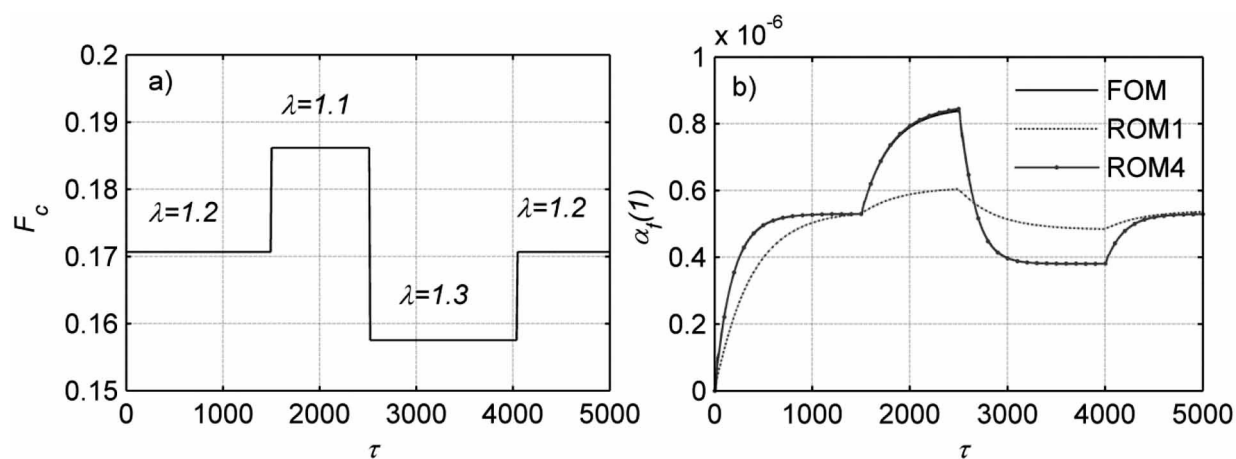


Fig. 6. Transient fuel feed rate (a) and response of fine char concentration at the outlet obtained using FOM, ROM1 and ROM4 (b)

Eventually, the performance of ROM in transient operation is verified. As previously, the fuel feed rate is varied stepwise, now in time (Fig. 6a) and dynamic response of the ROM to this variation is evaluated. Figure 6b reports outlet values of the fine concentration obtained by means of FOM and two ROMs, both built from snapshots sets consisting 25 solution profiles. As expected, ROM1 fails completely in the determination of the dynamical response of the system, while the ROM build by the projection of the original FOM onto 4 modes (=14 ODE instead of initial 1502), follows accurately dynamic profile of fine char concentration at the combustor outlet.

## 5. SUMMARY AND CONCLUSIONS

This paper discusses a POD-based approach aimed at the construction of reduced order models, applied to an idealised model of isothermal CFBC. The results presented here show that both POD modes and associated eigenspectra can be highly sensitive to the number of realisations, called customarily *snapshots*, even

when determined from a relatively simple solution, from the point of view of spatiotemporal complexity. Nevertheless, as demonstrated in this study there is no direct correlation between the convergence of the eigenvalues (or eigenmodes) and the actual performance of the resulting ROM. This indicates that the only solid criterion for the choice of sampling policy remains the approximation error of the ROM. Furthermore, the possibility emerges of constructing a faithful basis from a very low number of observations, which could be of the great importance when applied to 2D or 3D problems, or when determining empirical modes from limited number of experimental observations. The method itself permits to reduce significantly, with no loss in the accuracy, the order of the original system and thus computational time, which is especially important in real-time control applications and for the detailed analysis of distributed dynamical models characterised by large number of operating parameters.

## SYMBOLS

|                       |  |
|-----------------------|--|
| <i>a</i>              | modal coefficient  |
| <b>C</b>              | autocorrelation matrix belonging to $\mathfrak{R}^M \times \mathfrak{R}^M$ |
| <i>d</i>              | particle diameter, m   |
| <i>E</i>              | cumulative correlation energy of basis functions                           |
| <i>F</i>              | dimensionless mass flow rate ( $= \hat{F}/F_{ref}$ )                       |
| $\hat{F}$             | mass flow rate, kg/s   |
| <b>K</b>              | autocorrelation matrix belonging to $\mathfrak{R}^N \times \mathfrak{R}^N$ |
| <i>H</i>              | height of the riser, m   |
| <i>N</i>              | number of gridpoints   |
| <i>M</i>              | number of snapshots  |
| <i>Q</i>              | dimensionless volumetric flow rate, ( $= \hat{Q}/Q_{ref}$ )                |
| $\hat{Q}$             | volumetric flow rate, m <sup>3</sup> /s                                    |
| <i>r</i>              | consumption rate due to combustion or attrition, s <sup>-1</sup>           |
| <i>S</i>              | cross section of the riser, m <sup>2</sup>                                 |
| <i>t</i>              | time, s  |
| <i>T</i>              | temperature, K   |
| <i>u</i>              | velocity, m/s  |
| <i>v</i>              | dimensionless velocity ( $= u/u_{ref}$ )                                   |
| <i>V</i>              | loop-seal volume, m <sup>3</sup>   |
| <i>α</i>              | dimensionless suspension density ( $= \rho/\rho_{ref}$ )                   |
| <i>ε</i>              | voidage  |
| <i>φ</i>              | POD basis function   |
| <i>κ</i> <sub>1</sub> | dimensionless parameter in Eq. (3) ( $= F_{c,ref}/(u_{ref}\rho_{ref}S)$ )  |
| <i>κ</i> <sub>2</sub> | dimensionless parameter in Eq. (5) and Eq. (6) ( $= V/HS$ )                |
| <i>λ</i>              | excess air factor or POD eigenvalue  |
| <i>η</i>              | cyclone efficiency   |
| <i>ρ</i>              | suspension density, kg/m <sup>3</sup>                                      |
| <i>σ</i>              | dimensionless consumption rate ( $= rH/u_{ref}$ )                          |
| <i>τ</i>              | dimensionless time ( $= tu_{ref}/H$ )                                      |

### *Subscripts*

|             |                                |
|-------------|--------------------------------|
| <i>0</i>    | refers to superficial velocity |
| <i>a</i>    | refers to attrition            |
| <i>b</i>    | refers                         |
| <i>c</i>    | refers to coarse char          |
| <i>f</i>    | refers to fine char            |
| <i>prim</i> | refers to primary air          |

|            |                           |
|------------|---------------------------|
| <i>rec</i> | refers to recycled solids |
| <i>ref</i> | refers to reference value |
| <i>sec</i> | refers to secondary air   |
| <i>tot</i> | refers to total           |

## REFERENCES

- Barletta D., Marzocchella A., Salatino P., Kang S.G., Stromberg P.T., 2003. Modelling fuel and sorbent attrition during circulating fluidized bed combustion of coal. *17th International Fluidized Bed Combustion Conference*. Jacksonville, USA, 18-21 May 2003, 341-351.
- Basu P., 1999. Combustion of coal in circulating fluidized-bed boilers: a review. *Chem. Eng. Sci.*, 54, 5547-5557. DOI: 10.1016/S0009-2509(99)00285-7.
- Bizon K., Continillo G., 2009. Formulation and spectral reduction of the dynamical model of a circulating fluidized bed combustor. *Chem. Prod. Process Model.*, 4, 1934-2659. DOI: 10.2202/1934-2659.1416.
- Bizon K., Continillo G., Lombardi S., Merola S.S., Sementa P., Tornatore C., Vaglieco B.M., 2010. Analysis of flame kinematics and cycle variation in a port fuel injection spark ignition engine. *SAE Int. J. Engines*, 2, 443-451.
- Bizon K., Continillo G., 2012. Reduced order modelling of chemical reactors with recycle by means of POD-penalty method. *Comput. Chem. Eng.*, 39, 22-32 DOI: 10.1016/j.compchemeng.2011.10.001.
- Bizon K., Continillo G., Berezowski M., Smuła-Ostaszewska J., 2012. Optimal model reduction by empirical spectral methods via sampling of chaotic orbits. *Physica D*, 241, 1441-1449. DOI: 10.1016/j.physd.2012.05.004.
- Brenner T.A., Fontenot R.L., Cizmas P.G.A., O'Brien T.J., Breault R.W., 2012. A reduced-order model for heat transfer in multiphase flow and practical aspects of the proper orthogonal decomposition. *Comput. Chem. Eng.* 43, 68-80. DOI: 10.1016/j.compchemeng.2012.04.003.
- Breuer K.S., Sirovich L., 1991. The use of the Karhunen-Loève procedure for the calculation of linear eigenfunctions. *J. Comput. Phys.* 96, 277-296. DOI: 10.1016/0021-9991(91)90237-F.
- Hekmati A., Ricot D., Druault P., 2011. About the convergence of POD and EPOD modes computed from CFB simulation. *Comput. Fluids*, 50, 60-71. DOI: 10.1016/j.compfluid.2011.06.018.
- Hesthaven J.S., Gottlieb S., Gottlieb D., 2007. *Spectral methods for time-dependent problems*. Cambridge University Press, Cambridge, 117-123; 153-160.
- Holmes P., Lumley J.L., Berkooz G., 1996. *Turbulence, coherent structures, dynamical systems and symmetry*, Cambridge University Press, Cambridge, 88-100.
- Lombardi S., Bizon K., Marra F.S., Continillo G., 2013. Optimization of design parameters of a Stirling generator for use with a fluidized bed combustor. *Int. J. Thermodyn.*, 16, 155-162. DOI: 10.5541/ijot.472.
- Lu B., Zhang N., Wang W., Li J., Chiu J.H., Kang S.G., 2013. 3-D full-loop simulation of an industrial-scale circulating fluidized-bed boiler. *AIChE J.*, 59, 1108-1117. DOI: 10.1002/aic.13917.
- Lucia D., Beran P.S., Silva W., 2003. Reduced-order modeling: new approaches for computational physics. *Prog. Aerosp. Sci.*, 40, 51-117. DOI: 10.1016/j.paerosci.2003.12.001.
- Rajat G., Yogendra J., 2013. Error estimation in POD-based dynamic reduced-order thermal modeling of data centers. *Int. J. Heat Mass Transfer.*, 57, 698-707. DOI: 10.1016/j.ijheatmasstransfer.2012.10.013.
- Rowley C.W., Colonius T., Murray R.M., 2001. Dynamical models for control of cavity oscillations. *7th AIAA/CEAS Aeroacoustics Conference*. Maastricht, The Netherlands, 28-30 May 2001, 2001-2126.
- Sirovich L., 1987. Turbulence and the dynamics of coherent structures. I – Coherent structures. *Quart. Appl. Math.*, 45, 561-571.
- Zhang Y., Henson M.A., Kevrekidis I.G., 2003. Nonlinear model reduction for dynamic analysis of cell population models. *Chem. Eng. Sci.*, 58, 429-445. DOI: 10.1016/S0009-2509(02)00439-6.

Received 02 February 2015  
Received in revised form 11 August 2015  
Accepted 07 September 2015